Tunable compression of wind tunnel data

Antonio Possolo*

Statistical Engineering Division, Information Technology Laboratory, National Institute of Standards and Technology, U.S. Department of Commerce, Gaithersburg, Maryland, USA

Michael Kasperski

Department of Civil and Environmental Engineering Sciences, Ruhr-Universität Bochum, Bochum, Germany

Emil Simiu

Materials and Construction Research Division, Building & Fire Research Laboratory, National Institute of Standards and Technology, U.S. Department of Commerce, Gaithersburg, Maryland, USA

(Received April 14, 2009, July 9, 2009)

Abstract. Synchronous wind-induced pressures, measured in wind-tunnel tests on model buildings instrumented with hundreds of pressure taps, are an invaluable resource for designing safe buildings efficiently. They enable a much more detailed, accurate representation of the forces and moments that drive engineering design than conventional tables and graphs do. However, the very large volumes of data that such tests typically generate pose a challenge to their widespread use in practice. This paper explains how a wavelet representation for the time series of pressure measurements acquired at each tap can be used to compress the data drastically while preserving those features that are most influential for design, and also how it enables incremental data transmission, adaptable to the accuracy needs of each particular application. The loss incurred in such compression is tunable and known. Compression rates as high as 90% induce distortions that are statistically indistinguishable from the intrinsic variability of wind-tunnel testing, which we gauge based on an unusually large collection of replicated tests done under the same wind-tunnel conditions.

Keywords: wind tunnel testing; data compression; pressure taps; wind loads; bending moments; wavelet representation; wavelet thresholding; extreme values.

1. Introduction

To design buildings capable of withstanding specified wind effects, while minimizing construction costs and materials consumption, requires measuring aerodynamic pressures in specialized wind tunnels that simulate atmospheric flows, and then deriving the corresponding forces and bending

* Chief, Corresponding Author, E-mail: antonio.possolo@nist.gov

moments that are induced in the building's structure.

Since those pressures are highly variable in time and space, not only do the model buildings used in these wind-tunnel tests typically have to be instrumented with hundreds of pressure taps, but the periods of wind-on also have to be sufficiently long to capture all the characteristics of the airflow likely to impact building performance.

These wind-tunnel tests typically generate datasets so large that their storage and transmission is challenging for many potential users. However, enabling use of digital wind-tunnel data, as opposed to the conventional pressure tables and plots included in engineering standards and codes, which in many cases have been developed from measured data merely based on informed judgment rather than on rigorous analysis, is key to designing safe buildings efficiently.

Recent calculations (Coffman, *et al.* 2009, Ho, *et al*. 2005, St. Pierre, *et al*. 2005) have shown that differences between bending moments induced in knees of portal frames by pressures specified for low-rise buildings in the ASCE 7 Standard on the one hand, and by pressures measured at the University of Western Ontario on the other, can be as high as ±50%. These differences arise in large part because code values summarize vast numbers of quantitative measurements into just a few values, which inevitably distorts the representation of the aerodynamic pressures, and can result in significant over-or underestimation of the effects that the actual pressures induce.

Therefore, to avoid the induced distortion of reality, one should strive to use the measured pressures directly in the process of building design, instead of relying on overly reductive surrogates thereof. Data storage and computational capacities have now advanced to a degree that makes this approach practical. This was recognized by the ASCE 7 Standard committee, which already allows the direct use of measured aerodynamic data in design and is expanding access by designers to large aerodynamic pressure databases.

The National Institute of Standards and Technology (NIST) has commissioned a database of aerodynamic pressures, covering low-rise industrial buildings of various dimensions, from the University of Western Ontario, which is available at http://www.nist.gov/wind. NIST is also developing plans for the massive extension of this database. And software has been developed (Main 2007) that facilitates use of the database to design a wide class of structures, and that includes an automated procedure for interpolation between existing datasets so that the existing information can also be used to design buildings whose dimensions are intermediate between those documented in the database.

Wind-tunnel testing of a single model building can easily produce upwards of a billion individual measurements. Their sheer size may create substantial challenges to their transmission and analysis. Therefore, it is worthwhile to seek methods that (i) facilitate the storage and transmission of such data, (ii) enable the detection and selective use of those portions of the data that are most relevant to building design, and (iii) allow assessing and explicitly controlling the errors inherent in the calculations.

The purpose of this paper is to report on the development of data reductions based on wavelet theory. While wavelets have been used in thousands of applications in numerous fields, including civil engineering and wind engineering, their application in support of aerodynamic database-assisted design is new. The paper explains how the compression scheme it proposes facilitates incremental data transmission tailored to the accuracy requirements of engineering design.

Some background is provided on wind-tunnel testing, the calculation of internal forces from the aerodynamic database, and a characterization of the uncertainties inherent in the calculation of the internal forces. A description of a proposed approach to data compression is then presented, and errors inherent in that approach are discussed within the context of the overall errors in the calculation of the engineering quantities of interest.

2. Wind-tunnel testing

Fig. 1 shows a typical wind tunnel model instrumented with pressure taps. For each wind direction (or, equivalently, the model being placed on a rotating table, for each orientation of the model with respect to the mean flow velocity), records are taken of the simultaneous time histories of the pressures at each tap. The data obtained from a rigid model with one specific geometry can be used for different structural systems: for example, hinged support, fixed support, or 3-pin-jointed frame. Furthermore, the ratio of the stiffness of rafter and column may be varied.

To achieve similarity between the wind tunnel modeling and the prototype situation it is desirable that the ratio between the geometric scales in the wind tunnel and in the prototype be equal to the geometric model scale. In our case the model scale was 1:275, and the integral length scale at building height of 40 mm is 350 mm. Achieving such a ratio of integral turbulence scales is difficult; however, a ratio that is two to three times smaller than the corresponding geometric scale is commonly accepted.

The data used in this study consists of measurements of pressures at 18 taps placed along the center bay of a low-rise building model, made in the wind-tunnel of Ruhr-Universität Bochum (Bochum, Germany) (Kasperski, *et al*. 1996), sampled at 1600 Hz, over 100 time periods, each equivalent to 1 full-scale storm-hour, and all with the same wind-flow direction. The building had height h to span d ratio $h/d = 0.4$, with full-scale size $h = 11$ m, and roof slope 5° (Fig. 2).

The responses are bending moments at the knees of a steel portal frame with hinged supports. The stiffness of the frame's rafter was assumed to be equal to the stiffness of the two columns. All pressures are normalized with respect to the mean velocity pressure at height h. The bending moments are obtained as follows: $M = \frac{1}{2}\rho v^2 C_M h^2 d$, where ρ, v, C_M, h and d denote the specific mass of air, the design velocity, the non-dimensional moment coefficient, the eave height, and the distance between frames, respectively. If ρ, v, h, and d are expressed in kg/m^3, m/s, m, and m, respectively, then M is expressed in Nm.

Each series of measurements made at each tap in the course of a single wind-tunnel run (equivalent to 1 full-scale storm-hour approximately) comprises 49,152 C_p values: in each such run the fan was started and adjusted to the appropriate velocity, pressures were measured, and then the fan motor was stopped. Since there are 18 taps and 100 such runs, the whole dataset comprises 88,473,600 values, consuming about 675 megabytes of electronic storage space.

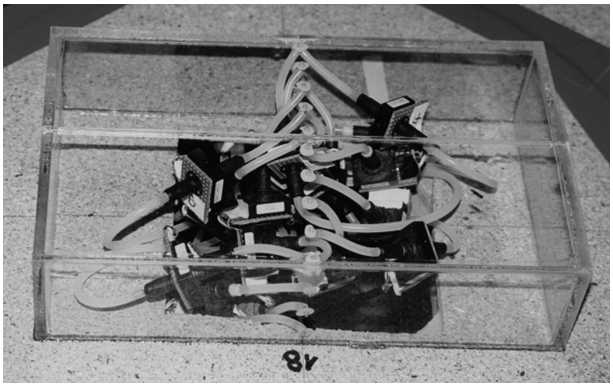

Fig. 1 Wind tunnel model. Constructed of Plexiglas, instrumented with pressure taps, and showing the corresponding tubing that connects them to differential pressure transducers.

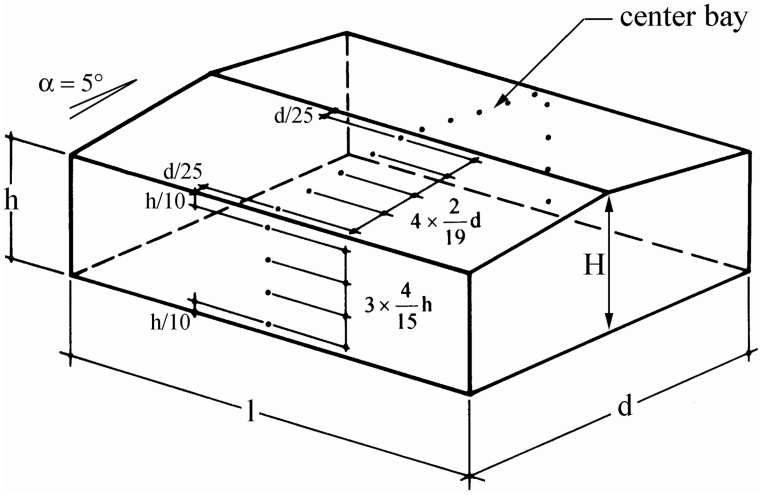

Fig. 2 Test Frame. Schematic arrangement of 18 taps along the center bay of a low-rise building model with $h/d = 0.4$, where $h = 11$ m in full scale, and roof slope 5°.

The time series have all been filtered digitally because, in the wind tunnel, the pressure sensors will measure not only the pressure fluctuations which are induced by the velocity fluctuations, but also the effects of any acoustic noise in the tunnel. For model tests on low-rise buildings, the noise in this particular tunnel is fairly large relative to the signal. There are several sources of noise: a standing wave in the wind tunnel, which gives an isolated peak in the frequency content; the motor and mechanisms that drive the fan; and the fan itself.

By and large, the noise contributions can be classified into two categories. The first comprises low to mid-frequency components with amplitude that remains approximately constant over the tunnel's cross-section: their contributions are eliminated during data pre-processing by measuring the pressure on the floor and subtracting this measured value from all the measurements made by the pressure taps on the model building. Although this removes the low-frequency and most of the mid-frequency noise, it exacerbates the high-frequency components of the noise.

The noise from the fan dominates the second category. The corresponding pressure fluctuations are synchronized with the fan's rotation, and can be described by a combination of harmonic and probably sub-harmonic waves. The amplitude of this noise component depends on the distance between the taps and the fan's axis, and on the fan's upstream distance to the taps.

The most efficient way of removing the fan noise is to have sound absorbers around the fan. Since this tunnel does not have such insulation, a digital filter was applied instead.

3. Internal forces & bending moments

Internal (shear and axial) forces and bending moments result from internal stresses at various cross-sections of structural members, and are produced by external loads applied on the building of interest. This note considers only wind-induced loads. At each time t the wind induces at each pressure tap a wind force approximately equal to the pressure at that tap multiplied by the tap's tributary area.

If the structure is linearly elastic, for any specified cross-section of a structural member the internal force at time t is approximately equal to the sum, over all taps affecting that member, of the wind forces acting at the taps multiplied by the respective influence coefficients (an influence coefficient is the internal force induced at the cross-section under consideration, by a unit force acting at a tap in a direction normal to the building envelope).

For design purposes, it is the peaks (up or down) of the time series of the internal forces that are of primary interest. The probability distributions of the peaks can be obtained using the methods discussed under item III-B at www.nist.gov/wind, for example. Rigato, *et al.* (2001), Simiu and Miyata (2006), Main and Fritz (2006), and Duthinh, *et al.* (2008) describe methods to account for the effects of wind directionality at a site.

For our test conditions, as illustrated in Fig. 2, the ratio between (a) the bending moment at time t during wind-tunnel run i=1,..., 100, and (b) the velocity pressure for each of the two knees of the frame, is obtained as $\Sigma_{j=1}^{18} C_p(i,j,t)I(j)$, where $C_p(i,j,t)$ denotes the value of the pressure coefficient measured at time t by tap j in the ith run, and $I(j)$ is the influence coefficient for tap j on the particular knee of interest.

4. Variability of bending moments

The values of the bending moments vary both within each run, and between runs. The between-runs variability provides a standard against which one should assess the severity of any loss of information that a data compression scheme may incur: indeed, if the compression is lossy (that is, some information gets lost in the process), but the corresponding degradation of the signal that results from a compression-uncompression cycle is comparable to the variability between-runs, then the degradation arguably is practically insignificant.

This variability, which is due to the vagaries of wind-tunnel testing, provides only a lower bound on the uncertainty of the bending moments. Other participating sources of uncertainty (whose contributions we will not attempt to quantify in this study) include: the analog-to-digital converter, the measurement of the reference pressure, the determination of the tap locations, and the computation of the influence coefficients.

To begin to quantify the components of variability of the bending moments that are attributable to the vagaries of wind-tunnel testing, we fitted a linear, Gaussian mixed-effects model (Pinheiro and Bates 2000) to the 15% trimmed mean of the values of the bending moment over each interval of duration 1 full-scale minute (comprising 819 measurements), at each knee of the frame separately. (The 15% trimmed mean of a batch of numbers is obtained by discarding the smallest 15% and the largest 15% of the batch, and then averaging the rest.) The models were fitted to the data using function lme of the nlme package (Pinheiro, *et al.* 2008) for the R environment for statistical computing (R Development Core Team 2008).

We chose that summary statistic, the 15% trimmed mean, rather than the average or the median, to strike a felicitous compromise between resistance to outliers and most efficient summarization of the information in the data, and to ensure compliance with the assumptions that validate the statistical analysis just mentioned. (Different but nearby values of the trimming percentage lead to similar results.)

The between-run variability was about 5 times larger than the within-run variability at one of the frame's knees, and it was about 2 times larger at the other. At both knees, the component of the

standard uncertainty corresponding to between-run variability amounted to about 2.5% of the typical value of the bending moment. And if the analysis focuses on the maximum absolute value of the bending moment over the same 1 full-scale minute intervals, then this becomes 5.5%.

Since this is a lower bound on the uncertainty, any distortion resulting from data compression that is comparable to this uncertainty is inconsequential.

In our opinion, an error of approximately 5% due to the data compression is therefore acceptable. Parenthetically we note that an international comparison of wind tunnel estimates of wind effects on low-rise buildings (Fritz, *et al.* 2008) shows that the peak moments in a frame section near the knee joint typically varied by more than 10% when the same structure was tested in different tunnels.

5. Representation

The sheer volume of data that wind-tunnel testing typically generates poses a challenge to the dissemination and practical use of the invaluable information that they hold. Data compression should alleviate the difficulties that these datasets create, but only if it manages to reduce data volume by more than one order of magnitude, while still preserving the features of the time series of pressures that are critical for building design: in particular, the largest excursions in value that are likely to induce extreme values of the internal forces and bending moments that act upon the supporting structures.

In addition, it is desirable that the compression mechanism should data transmission by allowing meaningful discretization and stratification of the information in the data: in other words, the representation of the compressed data should be such that it comprises mutually orthogonal packets whose natural ordering is such that successive packets merely refine what preceding packets have conveyed already. In this way, it is possible to increase the accuracy of the signal's representation incrementally, as circumstances may demand, without having to retransmit what has been sent already.

The test that is the focus of our attention here is of modest size, when compared with wind-tunnel tests of model buildings that are instrumented with hundreds of taps, measuring pressures at high data rates (500 Hz being typical): modest as it may be, already it produced about 88 million measurements of C_p.

Fig. 3 shows a segment of the time series of C_p values measured at tap 3, close to the end of run 48. The pattern that it exhibits is fairly typical: the fluctuations do not suggest any obvious periodicity, and are dominated by occasional sharp spikes (up or down) of very short duration, against a background of oscillations that may drift over time, in level, amplitude and frequency.

On the one hand, since the pressures measured by the taps are integrated to compute forces and moments, any compression procedure must preserve the phase relations between the signals measured by different taps. On the other hand, some signal loss may be tolerable because only the largest pressure excursions are likely to induce extreme forces and moments, which drive the design of the building's structure.

The discrete Fourier transform (Percival and Walden 1993, Oppenheim, *et al.* 1999) affords a representation that certainly possesses the orthogonality alluded to above, whereby the signal is decomposed into sinusoidal oscillations of different frequencies (and amplitudes, and phases). It does, however, suffer from two shortcomings in the context of our application: (i) if the signal is not stationary, then the Fourier representation may require an unwieldy large number of sinusoidal

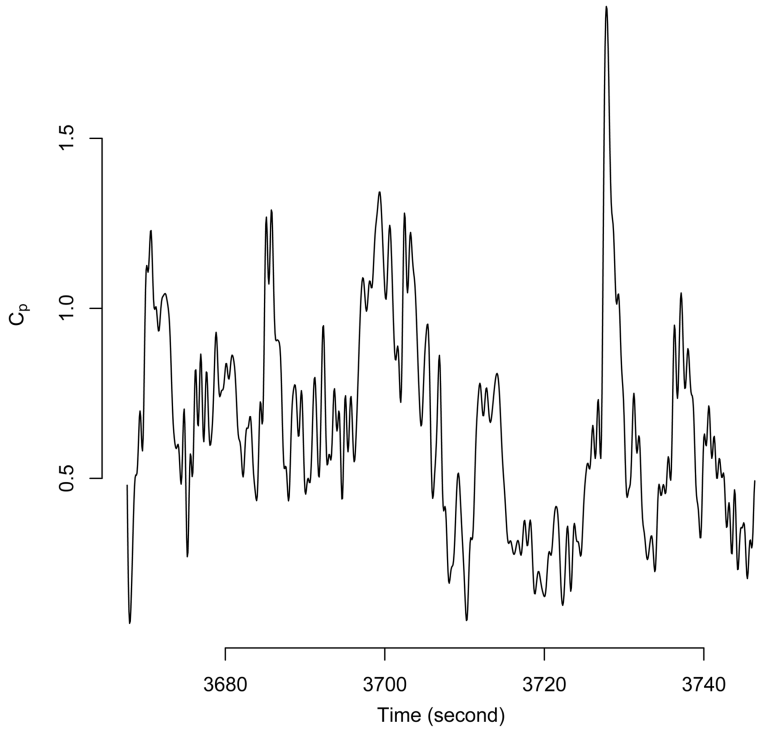

Fig. 3 C_p Fluctuations. Trace of 1,024 consecutive C_p values measured at tap 3, close to the end of run 48, shows a typical pattern: the fluctuations have no obvious periodicity, and are dominated by occasional sharp spikes (up or down) of very short duration, against a background that may drift over time.

components; (ii) if the signal is markedly non-periodic, possibly displaying occasional spikes, then the Fourier transform similarly struggles to represent these temporally isolated occurrences.

The wavelet representation (Mallat 1989), instead, seems tailor-made for our situation because it naturally adapts to signals with patterns that are prevalent in our data. It achieves this by using a functional template (the so-called mother wavelet) that it then dilates and translates to produce a collection of basis functions for the signal, in a manner that parsimoniously represents features that are localized in time, and whose frequency content also lies within particular, narrow bands – (Percival and Walden 2000, Gençay, *et al*. 2002).

Fig. 4 shows the components of an additive decomposition (multiresolution analysis (Percival and Walden 2000)) of the time series of C_p values depicted in Fig. 3: each of those components is a projection onto the wavelet basis, and reveals how this time series varies at a particular scale. The decomposition was computed using function mra of the package waveslim (Whitcher 2007) for the R environment for statistical computing (R Development Core Team 2008).

The wavelet representation possesses these distinctive attributes: (i) a very small number of coefficients suffice to delineate the principal features of the time series, even when this series is far from stationary; (ii) the components that it produces can be transmitted and added in sequence until the cumulative sum achieves the required representational accuracy. The first allows very efficient compression, and the second makes the compression process tunable (that is, one can choose the target compression ratio).

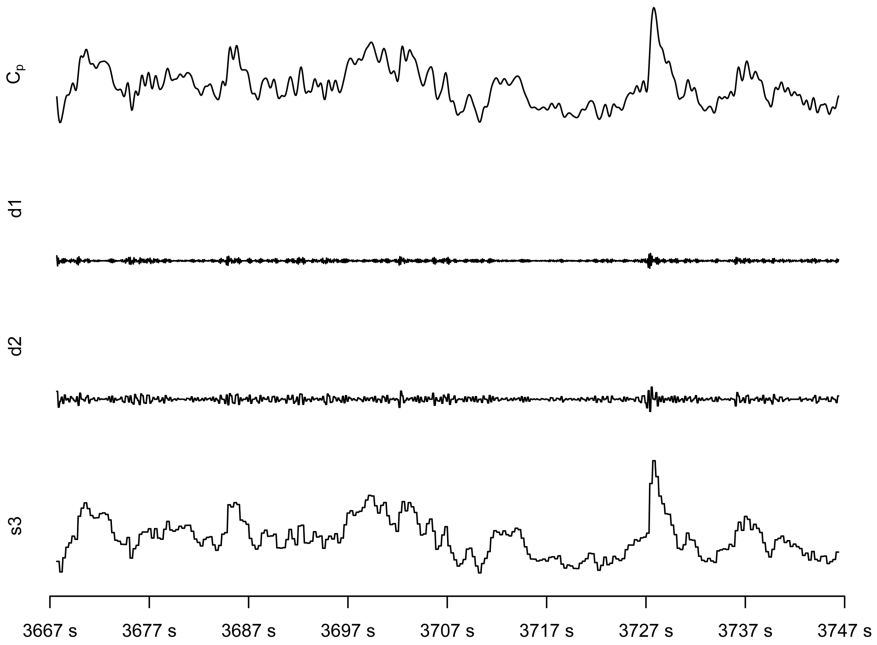

Fig. 4 Multiresolution analysis of C_p series. Additive wavelet decomposition of the time series of C_p values depicted in Fig. 3, computed using function mra of the package waveslim (Whitcher 2007) for the R environment for statistical computing (R Development Core Team 2008). The discrete wavelet transform used the Haar wavelet (Daubechies 1992) and periodic boundary conditions (Gençay, *et al.* 2002), and the analysis was carried out to depth 2: this expresses the observed C_p values as the sum of a "smooth" (s3) and two levels of "detail" (d1 and d2). The four panels have the same vertical scale, which is labeled in Fig. 3.

6. Compression

The discrete wavelet transform of a time series of C_p values is defined by the mother wavelet, and by the corresponding wavelet coefficients (of which there are as many as there are data points in the series). The preceding discussion of multiresolution analysis suggests that a simple compression scheme amounts to treating as zero all wavelet coefficients whose absolute value is smaller than a suitably chosen threshold $\tau > 0$: then all one needs to keep are the values of those coefficients that are greater than t in absolute value, and also the indexes that indicate their position in the sequence of coefficients. Thresholding (Donoho and Johnstone 1994) has been widely used in many applications, including in structural engineering (Gurley and Kareem 1999). Our compression procedure consists of the following two steps, which must be applied to the series of C_p values measured at each tap:

- **Step 1:** Compute the discrete wavelet transform of the data series, using a selected mother wavelet and a specified number of levels of detail for the corresponding multiresolution analysis, and adopting a particular policy to deal with boundary effects (we use periodic boundary conditions throughout this study);
- **Step 2:** Define the threshold τ as the 100(1-2α)th percentile (for $0 < \alpha < ¼$) of the absolute values of the wavelet coefficients, and set all wavelet coefficients to 0 whose absolute value is less than or equal to τ.

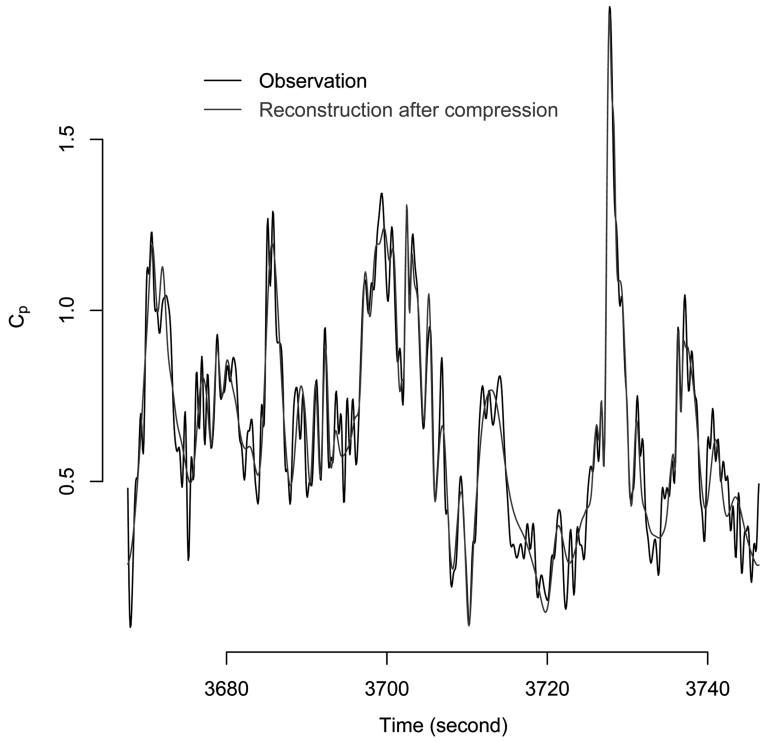

Fig. 5 Reconstruction of C_p series after compression. The black line depicts the same series of 1,024 C_p values that was introduced in Fig. 3, and the red line depicts the series that obtains after compression and reconstruction from the compressed series, performed as explained in §6. In this case, the effective compression rate was 90%, the maximum reconstruction error was 0.25 (13% of the maximum C_p value), and the root mean squared reconstruction error was 0.078 (4% of the maximum C_p value).

The compressed series is then stored as its τ-thresholded wavelet representation, which comprises the non-zero wavelet coefficients, and their indexes (so that one will know where the non-zero coefficients should be placed in the sequence of wavelet coefficients that otherwise are 0, prior to reconstructing the series via the inverse wavelet transform): the effective compression rate is $100(1-\alpha)\%$.

Fig. 5 shows the result of reconstructing the series with 1,024 measurements depicted in Fig. 3 after 90% compression using the procedure just described, where the discrete wavelet transform consisted of 1 "smooth" and 9 levels of "detail", and was computed with Daubechies (1992) least asymmetric wavelet LA(20) and periodic boundary conditions (Gençay, *et al*. 2002). Since only 52 of the original 1,024 wavelet coefficients are greater than τ, the effective compression rate is $1-(2\times52/1{,}024) \approx 90\%$: the factor 2 that multiplies 52 accounts for the fact that, to perform the reconstruction, one needs to know not only the values of the non-zero wavelet coefficients, but also their positions in the vector of wavelet coefficients. Table 1 is included for the reader's convenience and presents the core of the corresponding compression procedure, as implemented in the R environment for statistical computing and graphics (R Development Core Team 2008) – comparably concise implementations are viable in other computational environments.

Table 1 R (R Development Core Team 2008) Implementation of tunable compression. The time series of C_p values is in vector *y*, depicted in both Figs. 3 and 5. Line 1 loads the waveslim R package (Whitcher 2007). Line 2 computes the discrete wavelet transform using Daubechies (1992) least asymmetric wavelet LA(20) and periodic boundary conditions (Gençay, *et al.* 2002). Line 3 computes the threshold *t* corresponding to the target compression ratio of 1-[2×(1−0.95)]=90%. Line 4 sets all the wavelet coefficients to 0 that are less than τ in absolute value. Line 5 applies the inverse discrete wavelet transform to the result, producing the time series *ys* reconstructed from the compressed data, which Fig. 5 depicts alongside *y*

1	library(waveslim)
2	y.dwt = dwt(y, wf="la20", n.levels=9, boundary="periodic")
3	tau = quantile(abs(unlist(y.dwt)), probs=0.95)
4	for (jL in 1:nL) {y.dwt[[jL]][abs(y.dwt[[jL]]) < tau] = 0}
5	ys = idwt(y.dwt)

7. Performance assessment

The LA(20) mother wavelet was selected for the illustration presented in §6 because it outperformed many other alternatives in a comparative study that assessed the maximum absolute error and the root mean square error in the reconstructions that they produced, for a 90% compression ratio.

However, in the context of database-assisted design the performance that matters is not so much the fidelity with which series of C_p values can be reconstructed from compressed data, but much more the accuracy that the compressed data achieve in reproducing the values of internal forces and bending moments.

Fig. 6 shows the extreme values of the moments observed over intervals of duration 20 full-scale minutes that correspond to the measured pressures, and to the pressures reconstructed after 90% compression.

The ordinates of the (blue) open circles are values of extreme moments corresponding to the measured pressures, and the ordinates of the (red) dots are values of the extreme moments corresponding to the pressures reconstructed after compression. The abscissae are the expected values of a sample of the same size, drawn from a generalized extreme value (GEV) distribution (Johnson, *et al*. 1995) fitted to the extreme moments corresponding to the measured pressures. Since the parameters of the best fitting GEV distribution are different before and after compression, the abscissae of the (blue) open circles typically are different from the abscissae of the (red) dots in the same panel.

The light-gray envelopes were built via Monte Carlo sampling, so that, with very high probability, 99.5% of the samples of the same size as those under consideration, and drawn from the best fitting GEV distribution, should yield points lying inside the envelope. Therefore, if the (red) dots lie between the upper and lower gray curves, then this suggests that the compression induced distortion that is statistically insignificant. This is obviously not the case for the minima at knee 1: here, however, the GEV model does not provide a good fit either to the moments corresponding to the measured, or to the compressed data.

The GEV includes the Gumbel, Fréchet and reversed Weibull distributions as special cases. For the maxima, the best fitting models were Gumbel, and for the minima they were reversed Weibull. The computations required to find the best-fitting GEV, using the method of maximum likelihood,

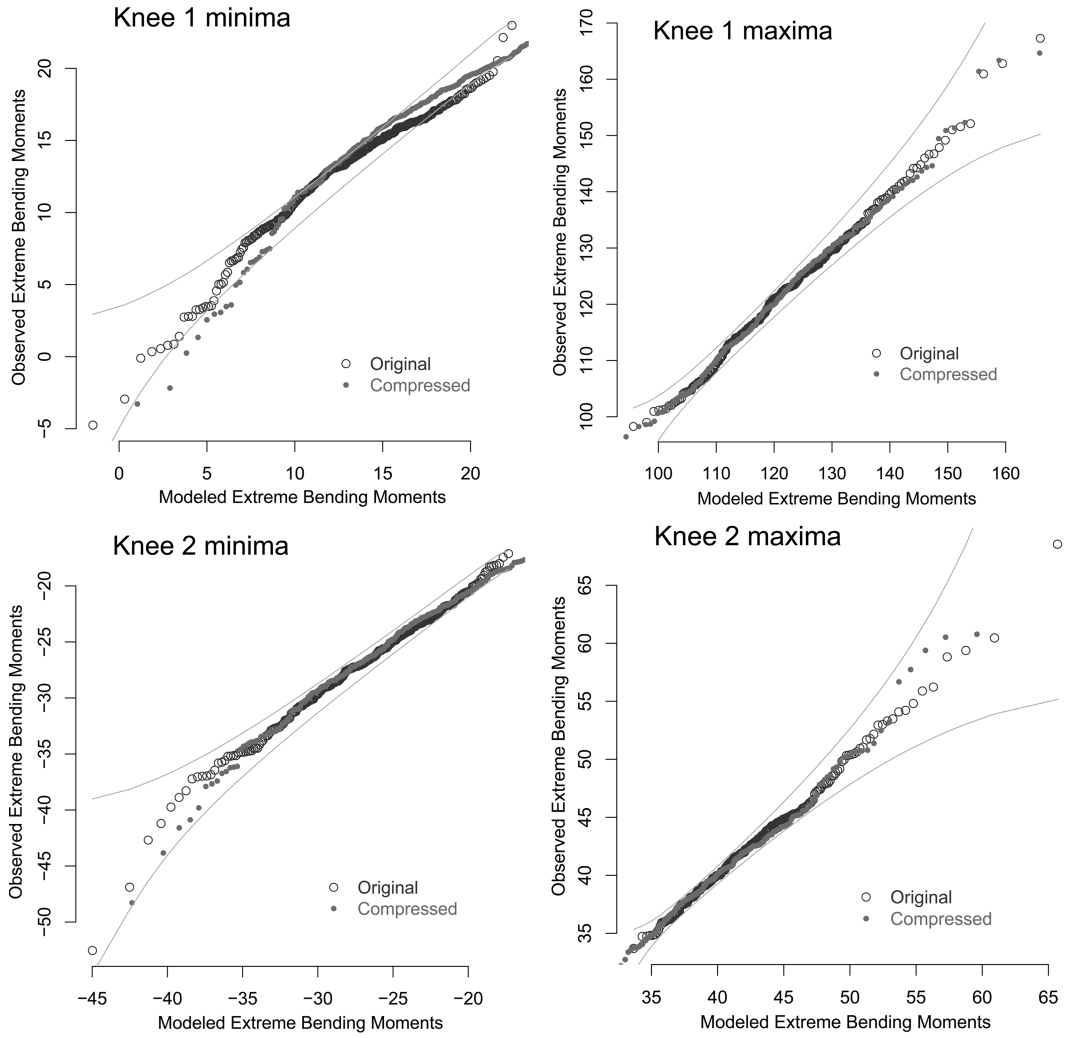

Fig. 6 Extreme bending moments before versus after compression. The ordinates of each plot are the observed extreme bending moments (in kNm) per unit of pressure (in kN/m^2) and unit of distance between frames (in m), for 20-min (full-scale) intervals. The abscissae are the expected values of a sample of the same size, drawn from a generalized extreme value (GEV) distribution fitted to the (blue) open circles, which correspond to the measured pressures. Since the parameters of the best fitting GEV distribution are different before and after compression, the abscissae of the (blue) open circles typically are different from the abscissae of the (red) dots in the same panel. The (red) dots correspond to the pressures reconstructed after 90% compression. The light-gray envelopes should enclose 99.5% of the samples, of the same size as those under consideration, that are drawn from the best fitting GEV distribution.

and to find the corresponding expected order statistics that are used as abscissae for the plots, all were done using facilities provided by package evd (Stephenson 2002) for the R (R Development Core Team 2008) programming environment for statistical modeling, data analysis, and graphics.

The maxima at knee 1 and the minima at knee 2 are decisive for the engineering design. The compression error is less than 5% for 98% of the maxima at knee 1, and for all of the minima at

knee 2 (in Germany, for example, a deviation of 5% of the total design value is widely accepted).

The largest discrepancy between original data and data reconstructed after compression occurs for the largest maxima at knee 2. It just so happens that, in this case, the maxima at knee 2 are not decisive drivers for design. However, even if they were critical, the corresponding design driver would not be the largest of the maxima (whose uncertainty typically is extremely large) but the 80^{th} percentile of such maxima, for which the compression-reconstruction cycle induces a difference of less than 5% relative to the corresponding value for the uncompressed data.

Also, as Fig. 6 shows, the samples of extreme moments corresponding to the compressed data are statistically indistinguishable from samples drawn from the GEV distributions that best fit the samples of extreme moments corresponding to the measured, uncompressed pressures.

8. Conclusions

For the reasons pointed out in §5, wavelet representations are better suited to approximate the characteristics of time series of pressure measurements that are likely to be consequential for building design than Fourier representations: in particular because the fluctuations in pressure tend not to suggest any obvious periodicity, and are dominated by occasional sharp spikes (up or down) of very short duration, against a background of oscillations that may drift over time, in level, amplitude and frequency.

Wavelet representations offer two important benefits: (i) drastically compressing wind tunnel data in a manner that preserves those features in the data that are most influential for building design; and (ii) facilitating incremental data transmission, in a way that is adaptable to the accuracy needs of each particular application.

Each series of measurements of pressure at each tap is compressed by replacing with zeros the values of all the wavelet coefficients whose absolute value is less than a particular threshold level, which is chosen to achieve a desired compression ratio. Once the intrinsic uncertainty of the C_p measurements is taken into account, which we have done based on replicated measurements made in the same tunnel, and on the results of an international intercomparison of wind-tunnel measurements, we show that wavelet-based compression by as much as 90% does not introduce significant distortion, relative to the complete wind-tunnel data, in the values of the bending moments that drive building design.

Acknowledgments

The authors thank Joseph A. Main and James Filliben (NIST, Gaithersburg, Maryland) for their comments and suggestions that led to substantial improvements of this contribution, and René Gabbai for his assistance during the early stages of this research.

References

Coffman, B.F., Main, J.A., Duthinh, D. and Simiu, E. (2009), "Wind effects on low-rise buildings: Database-assisted design vs. ASCE 7-05 Standard estimates", *J. Struct. Eng.*, in print.

Daubechies, I. (1992), *Ten Lectures on Wavelets*, CBMS-NSF Regional Conference Series in Applied Mathematics,

vol. 61, Society for Industrial and Applied Mathematics (SIAM), Philadelphia, PA.
Donoho, D.L. and Johnstone, I.M. (1994), "Ideal spatial adaptation by wavelet shrinkage", *Biometrika*, **81**(3), 425-455.
Duthinh, D., Main, J.A., Wright, A.P. and Simiu, E. (2008), "Low-rise steel structures under directional winds: Mean recurrence interval of failure", *J. Struct. Eng.*, **134**(8), 1383-1388.
Fritz, W.P., Bienkiewicz, B., Cui, B., Flamand, O., Ho, T.C.E., Kikitsu, H., Letchford, C.W. and Simiu, E. (2008), "International comparison of wind tunnel estimates of wind effects on low-rise buildings: Test-related uncertainties", *J. Struct. Eng.*, **134**(12), 1887-1890.
Gençay, R., Selçuk, F. and Whitcher, B. (2002), *An Introduction to Wavelets and Other Filtering Methods in Finance and Economics*, Academic Press, San Diego, CA. ISBN 0-12-279670-5.
Gurley, K. and Kareem, A. (1999), "Applications of wavelet transforms in wind, earthquake and ocean engineering", *Eng. Struct.*, **21**(2), 149-167.
Ho, T.C.E., Surry, D., Morrish, D. and Kopp, G.A. (2005), "The UWO contribution to the NIST aerodynamic database for wind loads on low buildings: Part 1. Archiving format and basic aerodynamic data", *J. Wind Eng. Ind. Aerod.*, **93**(1), 1-30.
Johnson, N.L., Kotz, S. and Balakrishnan, N. (1995), *Continuous Univariate Distributions*, vol. 2. John Wiley & Sons, New York, NY, Second edition.
Kasperski, M., Koss, H. and Sahlmen, J. (1996), "BEATRICE joint project: Wind action on low-rise buildings. Part 1. Basic and first results", *J. Wind Eng. Ind. Aerod.*, **64**(2), 101-125.
Main, J.A. (2007), "Database-assisted design of low-rise buildings for wind loads: Recent developments and comparisons with ASCE/SEI 7-05", *In R. Lyons, editor, Proc. of Sessions of the 2007 Structures Congress*, May 16-19, 2007, vol. 248, pages 11-11, American Society of Civil Engineers (ASCE), 2007, URL http://link.aip.org/link/?ASC/248/11/1.
Main, J.A. and Fritz, W.P. (2006), *Database-assisted design for wind: concepts, software, and examples for rigid and flexible buildings*, NIST Building Science Series 180, National Institute of Standards and Technology, Gaithersburg, Maryland, March 2006, http://www.itl.nist.gov/div898/winds/pdf_files/Main-Fritz_DAD_BSS180.pdf.
Mallat, S.G. (1989), "A theory for multiresolution signal decomposition: the wavelet representation", *IEEE T. Pattern Anal.*, **11**, 674-693.
Oppenheim, A.V., Schafer, R.W. and Buck, J.R. (1999), *Discrete-Time Signal Processing*, Prentice-Hall, Upper Saddle River, NJ, Second edition.
Percival, D.B. and Walden, A.T. (1993), *Spectral Analysis for Physical Applications: Multitaper and Conventional Univariate Techniques*, Cambridge University Press, Cambridge, UK.
Percival, D.B. and Walden, A.T. (2000), *Wavelet Methods for Time Series Analysis*, Cambridge University Press, Cambridge.
Pinheiro, J., Bates, D., DebRoy, S., Sarkar, D. and R Core Team (2008), *nlme: Linear and Nonlinear Mixed Effects Models*, URL http://www.r-project.org/,R package version 3.1-89.
Pinheiro, J.C. and Bates, D.M. (2000), *Mixed-Effects Models in S and S-Plus*, Springer-Verlag, New York, NY.
R Development Core Team (2008), R: *A Language and Environment for Statistical Computing*, R Foundation for Statistical Computing, Vienna, Austria, http://www.R-project.org, ISBN 3-900051-07-0.
Rigato, A., Chang, P. and Simiu, E. (2001), "Database-assisted design, standardization, and wind direction effects", *J. Struct. Eng.*, **127**(8), 855-860.
Simiu, E. and Miyata, T. (2006), *Design of Buildings and Bridges for Wind: A Practical Guide for ASCE-7 Standard Users and Designers of Special Structures*, John Wiley & Sons, Hoboken, NJ.
Stephenson, A.G. (2002), *evd: Extreme value distributions*, R News, **2**(2), 31-32, http://CRAN.R-project.org/doc/Rnews/.
St. Pierre, L.M., Kopp, G.A., Surry, D. and Ho, T.C.E. (2005), "The UWO contribution to the NIST aerodynamic database for wind loads on low buildings: Part 2. Comparison of data with wind load provisions", *J. Wind Eng. Ind. Aerod.*, **93**(1), 31-59.
Whitcher, B. (2007), *waveslim: Basic wavelet routines for one-, two-and three-dimensional signal processing*, http://www.r-project.org/,R package version 1.6.1.

JH